

Article

Comparison of FOSS4G Supported Equal-Area Projections Using Discrete Distortion Indicatives

Luís Moreira de Sousa * , Laura Poggio  and Bas Kempen 

ISRIC—World Soil Information, Droevendaalsesteeg 3, Building 101, 6708 PB Wageningen, The Netherlands

* Correspondence: luis.de.sousa@protonmail.ch

Received: 30 April 2019; Accepted: 7 August 2019; Published: 9 August 2019



Abstract: This study compares the performance of five popular equal-area projections supported by Free and Open Source Software for Geo-spatial (FOSS4G)—Sinusoidal, Mollweide, Hammer, Eckert IV and Homolosine. A set of 21,872 discrete distortion indicatives were positioned on the ellipsoid surface, centred on the cells of a Snyder icosahedral equal-area grid. These indicatives were projected on the plane and the resulting angular and distance distortions computed, all using FOSS4G. The Homolosine is the only projection that manages to minimise angular and distance distortions simultaneously. It yields the lowest distortions among this set of projections and clearly outclasses when only land masses are considered. These results also indicate the Sinusoidal and Hammer projections to be largely outdated, imposing too large distortions to be useful. In contrast, the Mollweide and Eckert IV projections present trade-offs between visual expression and accuracy that are worth considering. However, for the purposes of storing and analysing big spatial data with FOSS4G the superior performance of the Homolosine projection makes its choice difficult to avoid.

Keywords: FOSS4G; equal-area projection; Homolosine; EckertIV; Mollweide; Hammer; Sinusoidal; Discrete Global Grid

1. Introduction

In a relatively short span of time, the field of Geographic Information Systems (GIS) went from data wanton to data galore. The proliferation of Earth Observation programmes, coupled with the rising trend towards Open Data, has made a wealth of high quality, high resolution, globally covering data available to researchers and spatial data analysts. The sheer volume of data has become a challenge in itself. Today, data users must carefully consider storage and, more importantly, computation costs.

In the particular case of global rasters, analysts of big spatial data are often confronted with datasets provided in awkward map projections, that greatly increase demands on storage and computation. Table 1 compares the areas of the co-domain and land masses of various projections computed with GRASS [1]. These areas equate to the number of cells in a global raster with a cell side of 1 km. The Marinus of Tyre and Mercator projections, even though arguably the most popular projections in Earth Sciences today, impose massive overheads in storage space and computation time with the number of extra raster cells they require to discretise the surface of the globe. In order to minimise the size of the datasets and render them spatially representative of the surface of the Earth, big spatial data researchers often undertake as first task a re-projection with an equal-area projection.

The re-projection to an equal-area projection reduces the number of cells in the raster, which in theory leads to a loss of information (or spatial resolution). However, the raw datasets from which global data products are developed are primarily collected in the geodesic domain and therefore not subject to distortion. For example, the Moderate Resolution Imaging Spectrometer (MODIS) space-borne sensor managed by NASA collects images of the Earth in its bands 1 and 2 with cells of approximately 250 m in side (6.25 ha). Some of the products developed from this sensor are published

in the Marinus of Tyre projection with a cell side of 8 arc-seconds, meaning that at a latitude of 45° their area is down to 3.125 ha. At that latitude half of the cells in such raster are either interpolated or replicated from the raw data.

Table 1. Total areas of co-domain and land masses with different map projections.

Projection	Co-Domain (km ²)	Land Masses (km ²)
Equal-area	5.10×10^8	1.47×10^8
Robinson	5.12×10^8	1.56×10^8
Marinus of Tyre	8.00×10^8	2.65×10^8
Mercator ¹	2.77×10^9	1.20×10^9

¹ Domain limited to the latitude interval $[-89.5^\circ, 89.5^\circ]$.

If the need to store and compute datasets in an equal-area projection is obvious to big spatial data analysts, exactly how to do it may not be simple. In first place, the number of equal area projections supported by FOSS4G is rather limited, more so when solely considering those applicable globally. Since the late XX century, modern methods have been introduced, resulting in equal-area projections that address distance and angular distortions simultaneously [2]. However, these modern equal-projections do not find full support among the core FOSS4G libraries: *geographiclib* [3], *PROJ* [4] and *GDAL* [5]. Moreover, distortions that may result from the algorithmic implementations in these programmes are not simple to assess. Therefore, the choice of map projection in a big spatial data context supported by FOSS4G may not be straightforward.

There are few studies in the literature reporting software based comparisons of map projections, especially when considering the global scale. The study conducted by Seong et al. [6] is possibly the closest to address this question. However, these authors were primarily concerned with the loss and replication of cell values in categorical rasters when re-projected. These authors assessed four popular equal-area projections, that are common to this study: Sinusoidal, Mollweide, Eckert IV and Hammer. For their purposes, Seong et al. concluded that the Sinusoidal is the most performant. Two important caveats in this study should be taken into account: (i) the Gauss-Krüger projection was used as reference, not the geodetical domain, and (ii) the comparison was conducted within 52 small areas of 3 by 3 km spread randomly around the globe. This study can not be considered exhaustive and it is possible results would have been different had it been conducted globally. A final aspect: Seong et al. exclusively employed commercial software in their work.

Capek [7] evaluated an assortment of one hundred global projections using a benchmark composed by ratios of areal, angular and distance distortions, restricted to pre-set maxima. For each projection assessed, only the areas within which distortions remained below the pre-set maxima were used in the assessment. Setting this maxima implied that for each projection the area contributing to the comparison was different. Capek did not assess the performance of interrupted projections, like the Homolosine or the Eumorphic and also left out projections based on polyhedra, such as the Dymaxion or the equal-area projections developed by Snyder. Within equal-area projections Capek rated the Hufnagel X, developed in 1989, as the most performant. Such projection remains rare and is not supported by FOSS4G. Capek conducted his study using both computer and cartometric processing (depending on the projection). In some cases relevant differences are observed between the two computations.

Mulcahy and Clarke [8] reported a series of ten different methods used to portray distortions in map projections. Most of the methods inventoried are merely visual and may not be used in analytic comparisons. A distinct exception is Tissot's indicatrix which allows for analytic assessment and is visually expressive too. A few other methods beyond Tissot's indicatrix also allow both but their nature is similar, based on geometric structures. These authors further note that Tissot's indicatrix is most often used in discrete form and not as the infinitesimal ellipse originally proposed by Tissot.

This study addresses the question of selecting an appropriate equal-area projection supported by FOSS4G to optimise the storage and processing of big spatial data. The goal was to exhaustively measure angular and distance distortions across the globe for a series of candidate projections. These distortions

were assessed within a regular positioning framework, so that each area of the globe could have the same importance in the assessment. Considering that some global data only concern land, as is the case with soils or demographics, distortions over land masses were also assessed independently.

This article reports the process and results of this study. Materials and methods are laid out in Section 2, with results presented in Section 3. Section 4 reflects on these results and Section 5 closes with conclusions and future research directions.

2. Materials and Methods

2.1. Selected Projections

In previous work FOSS4G support was assessed for a series of equal-area projections [9]. In that earlier study support was defined as full implementation by FOSS4G sanctioned by the OSGeo Foundation, in particular the PROJ and GDAL libraries, plus the correct display of raster layers in cartography programmes (e.g., QGIS [10], gvSIG [11]). In general, the newer the projection the less likely it is to be supported. The pseudo-cylindrical projections developed around the turn of the XX century, like the series proposed by Eckert [12], are supported but many other relevant projections developed later, like the Eumorphic [13] or the polyhedral proposed by Snyder [2], are not implemented by any of the OSGeo sanctioned programmes.

Besides the somewhat popular Eckert IV, the only other relevant projection from the XX century supported by FOSS4G is the Homolosine, proposed by Goode [14]. Another relevant projection found to be fully usable is the one proposed by Hammer [15], which was developed in an attempt to address the extreme distortions at the edges of elliptical equal-area projections. Beyond these were also considered the centenary Sinusoidal projection (in use since at least the XVI century [16]) and the original elliptical projection developed by Mollweide at the beginning of the XIX century [16] and still popular today. The set of projections assessed in this study was thus defined as: Sinusoidal, Mollweide, Hammer, Eckert IV and Homolosine. Table 2 presents the corresponding PROJ strings. Other equal-area projections are supported by FOSS4G but do not present enough unique characteristics to set them markedly apart from the quintet analysed. The list of projections supported by PROJ can be accessed at <https://proj.org/operations/projections/index.html> (note that many of these are not supported by GDAL and/or GeoTools). Possibly avoiding mathematical complexity (and computation burden), software developers have favoured projections in the vein of those proposed around the turn of the XX century, with a single interruption and approachable formulations.

Table 2. PROJ strings used in this study.

Sinusoidal	+proj=sinu +lat_0=0 +lon_0=0 +datum=WGS84 +units=m +no_defs
Mollweide	+proj=moll +lat_0=0 +lon_0=0 +datum=WGS84 +units=m +no_defs
Hammer	+proj=hammer +lat_0=0 +lon_0=0 +datum=WGS84 +units=m +no_defs +wktext
Eckert IV	+proj=eck4 +lat_0=0 +lon_0=0 +datum=WGS84 +units=m +no_defs
Homolosine	+proj=igh +lat_0=0 +lon_0=0 +datum=WGS84 +units=m +no_defs

2.2. Discrete Indicatrices

The indicatrix proposed by Tissot [17] is a popular and effective method of depicting the distortions induced by a map projection. It features extensively in reference educational and technical textbooks [8,18]. The indicatrix is itself a simple object: an infinitesimal shape defined on the surface of the sphere or the ellipsoid. Usually, a series of indicatrices are positioned at regular intervals of latitude and longitude and are then projected onto the plane with different projections for visual comparison. Once projected, the shape, area and perimeter of the indicatrix changes. In conformal projections,

Tissot's indicatrices appear as circles, in pseudo-cylindrical equal-area projections they tend to acquire an elliptic shape.

In this study discrete constructions inspired on Tissot's indicatrix are used to compute distortion. Each discrete indicatrix is defined in the Geodetic domain as a shape of 1 km radius around a central point. From the central point of the indicatrix a set of four stems is developed, aligned with the four cardinal directions. Each of the four stems is 1 km long, being in fact a geodesic line (or loxodrome). This construction provides a discrete measure of distortion (i.e., non-analytic), than can thus be computed directly with common FOSS4G.

The geodesics composing the discrete indicatrices used in this study were computed with the `geographiclib` library, a cornerstone of FOSS4G, underlying many important packages (like PROJ). To compute a geodesic, `geographiclib` takes as inputs: (i) the coordinates of a starting point, (ii) an azimuth and (iii) a distance. The coordinates of the end point of the geodesic are the output. This computation is also referred to as the direct geodesic. For each indicatrix four geodesics are thus computed, all with the same starting point (the centre) and distance (1000 m) but with four different azimuths: 0° , 90° , 180° and 270° .

2.3. Discrete Global Grid

The positioning of the indicatrices used in this study is a crucial aspect to provide a balanced comparison of the five projections under analysis. It deals with two essential requirements: (i) guaranteeing that the comparison is not restricted to a single region of the globe and (ii) ensuring that every region of the globe (and of the projection co-domain) has a similar weight in the comparison. A comparison carried on a restricted region of the globe ignores the necessary spatial variation of deformations within the projection co-domain. In global cartograms, distortion indicatrices are often presented at regular intervals of latitude and longitude. This practice lends more weight to the indicatrices closer to the poles. In order to avoid such biases, distortions must be assessed across the entire geographic domain, or alternatively, following a regular discrete tessellation of the ellipsoid.

The indicatrices used in this study were positioned on the globe according to an hexagonal discrete global grid developed from the Snyder's icosahedral equal-projection. This kind of grid is commonly known as Icosahedral Snyder Equal-Area Grid (ISEAG) [19]. A discrete distortion indicatrix was positioned at the centre of each cell in this grid.

The software package `dggridR` [20] for the R programming language was used to create the ISEAG. This package wraps the ISEAG creation functions originally developed by Sahr in the C language. The grid was created with an aperture number of 3 and a resolution of 7, resulting in a cell area of 23 322 km². This translated into a total of 21,872 indicatrices positioned at an average distance of 165 km from their immediate neighbours.

2.4. Computation of Distortions

The discrete indicatrices described above were thus projected onto the plane with each of the five projections selected. Angular and distance distortions were computed as follows. The length of each indicatrix stem was computed and subtracted from the original 1000 m. The angles between the stems aligned with the North and South directions were obtained with Equation (1), whereas for the East and West directions Equation (2) was used. In these equations (s_p, s_m) are the cartographic coordinates of the stem end point and (c_p, c_m) are the coordinates of the indicatrix centre.

$$d_a = \arctan (s_m - c_m) / (s_p - c_p) \quad (1)$$

$$d_a = \arctan (s_p - c_p) / (s_m - c_m) \quad (2)$$

For each indicatrix four different angular distortions and four different distance distortions were obtained. Figure 1 summarises these computations visually.

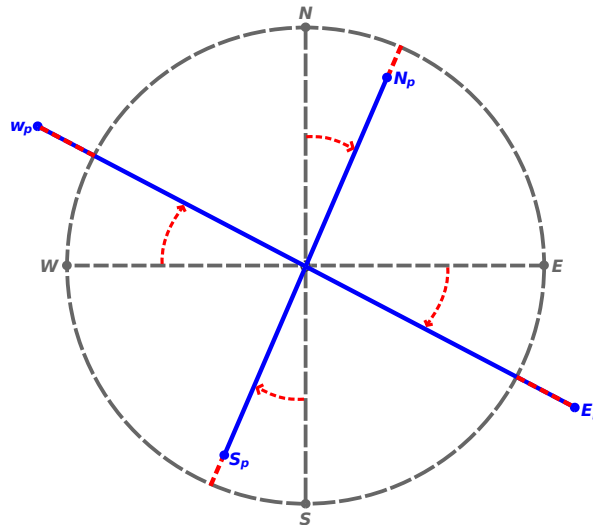


Figure 1. Graphical sketch of a projected discrete indicatrix. N_p , E_p , S_p and W_p represent the end points of the discrete indicatrix stems after projection; N , E and S , W represent their positioning if no distortion took place. The red segments and the red arc represent the distance and angular distortions computed.

3. Results

The distortion computation methods described above were implemented by a computer programme coded mostly in the Python language (R was used to interact with the `dggridR` library). The Python implementation of the `geographiclib` library greatly simplifies its use. The resulting programme is available at Codeberg (<https://codeberg.org/lde Sousa/projections-compare>) under an open source licence.

Figure 2 show boxplots of the absolute angular distortions for the five projections. Essential statistics for these distortion distributions are found in Table 3. The wide difference between the familiar RMSE and MAE metrics is due to a relevant number of outliers with high distortions (essentially the edges of the projection co-domain). Apart from the Hammer projection, all projections yield a mean angular distortion close to zero but between them the distribution is varied. The Homolosine and Eckert IV show the narrowest distributions, which reflects on the lowest mean absolute distortions. Concerning land masses alone, the distributions are somewhat similar to the global but in this case the Homolosine stands out more clearly with the lowest mean and tightest distribution. Figure 3 and Figure 4 convey the spatial distribution of angular distortion, showing mean absolute distortion at the location of each discrete indicatrix.

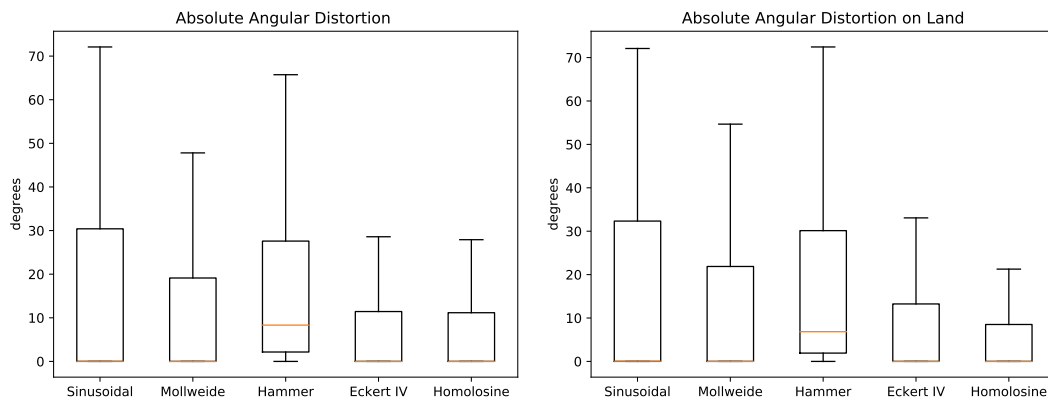


Figure 2. Box plots of absolute angular distortions (median in red).

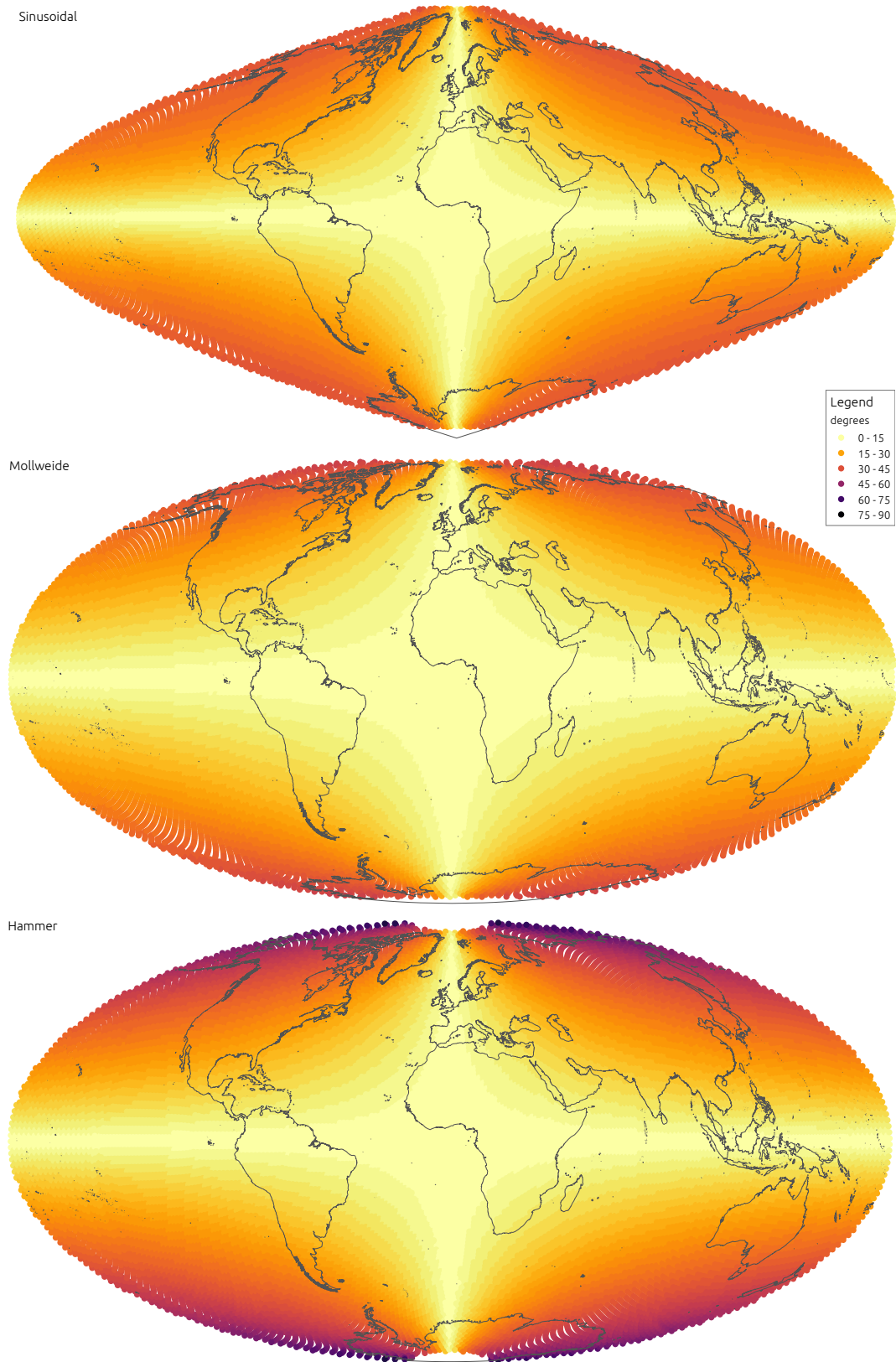


Figure 3. Mean absolute angular distortion at each indicatrix for the Sinusoidal, Mollweide and Hammer projections.

Table 3. Statistics for absolute angular distortions distributions.

(degrees)	Global			Land Masses		
	Mean	RMSE	MAE	Mean	RMSE	MAE
Sinusoidal	0	26.9	15.8	−1.4	26.7	15.5
Mollweide	0	22.8	12.3	−0.7	24.1	12.9
Hammer	0	27.1	17.7	−1.2	27.9	17.8
Eckert IV	0	17.4	8.7	−0.2	19.0	9.4
Homolosine	−1.2	15.4	7.9	−3.7	16.4	7.9

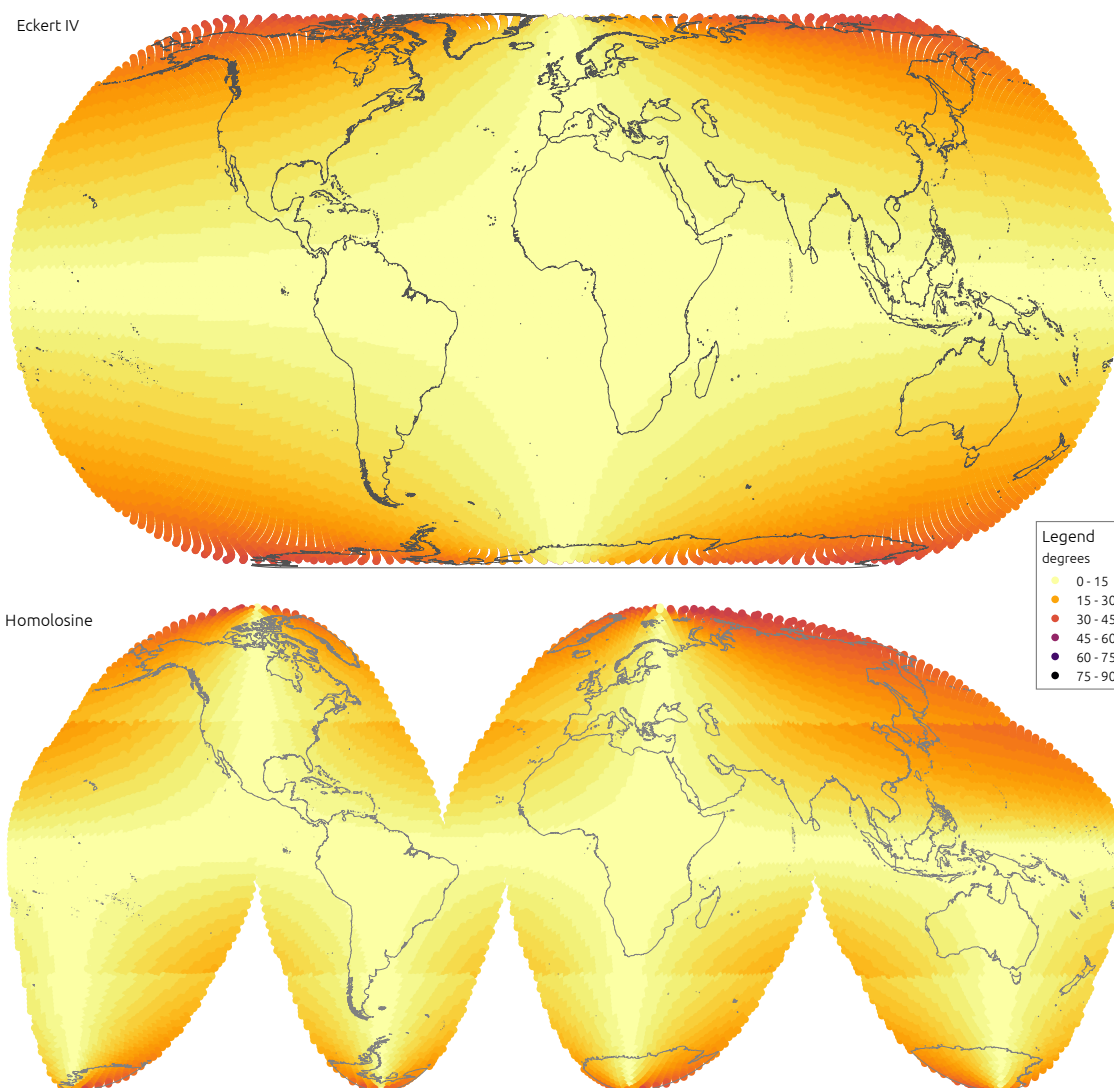
**Figure 4.** Mean absolute angular distortion at each indicatrix for the Eckert IV and Homolosine projections.

Figure 5 and Table 4 summarise distance distortions distributions. The rank is somewhat different for distances, with the Sinusoidal alone yielding a median close to zero. However, the narrowest distribution is the one obtained with the Homolosine, which also results in the lowest mean distortion. The distributions of distance distortions restricted to land masses are almost the same. But in this case the Homolosine yields distinctively the lowest mean and upper quantiles. Figures 6 and 7 display the spatial distribution of mean absolute distance distortions.

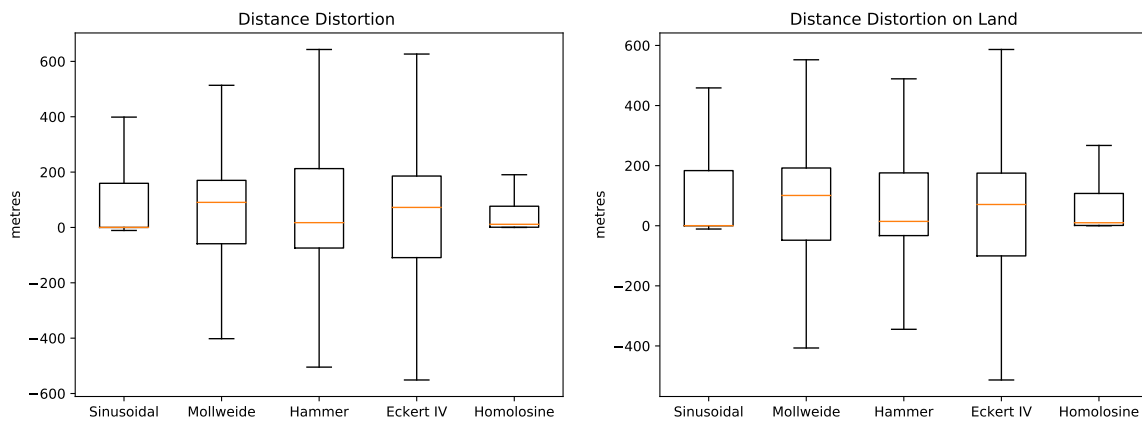


Figure 5. Box plots of distance distortions (median in red).

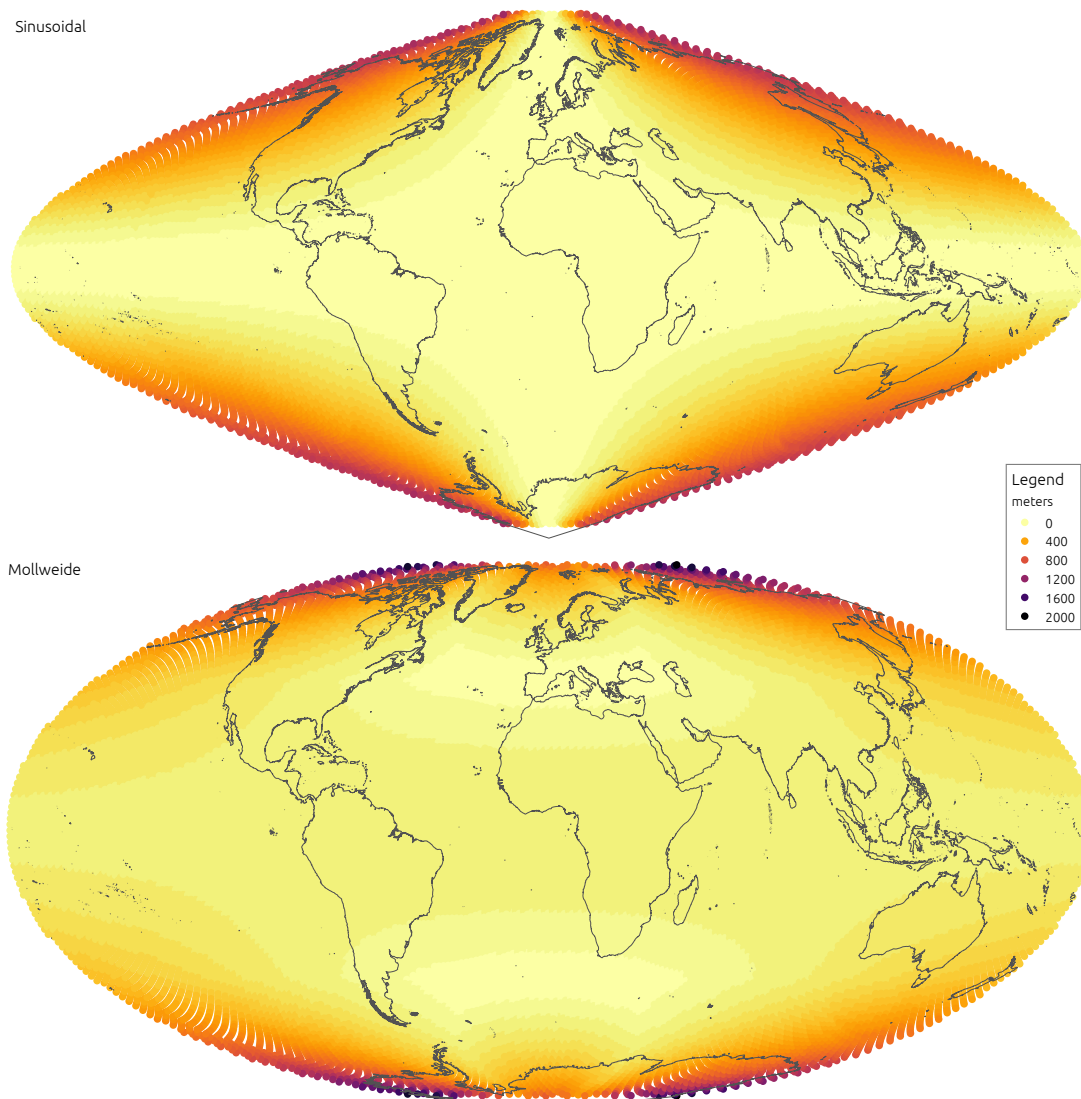


Figure 6. Cont.

Hammer

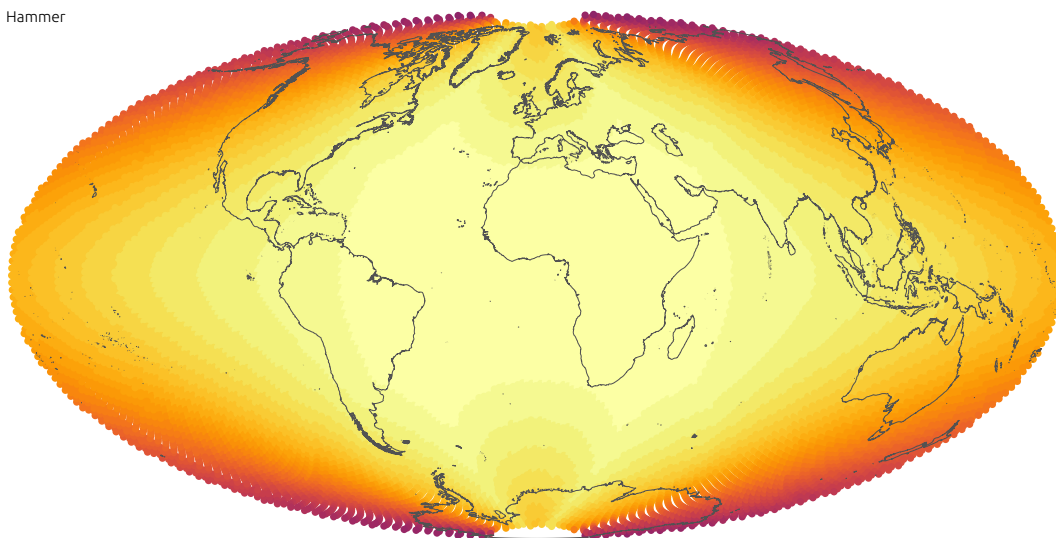
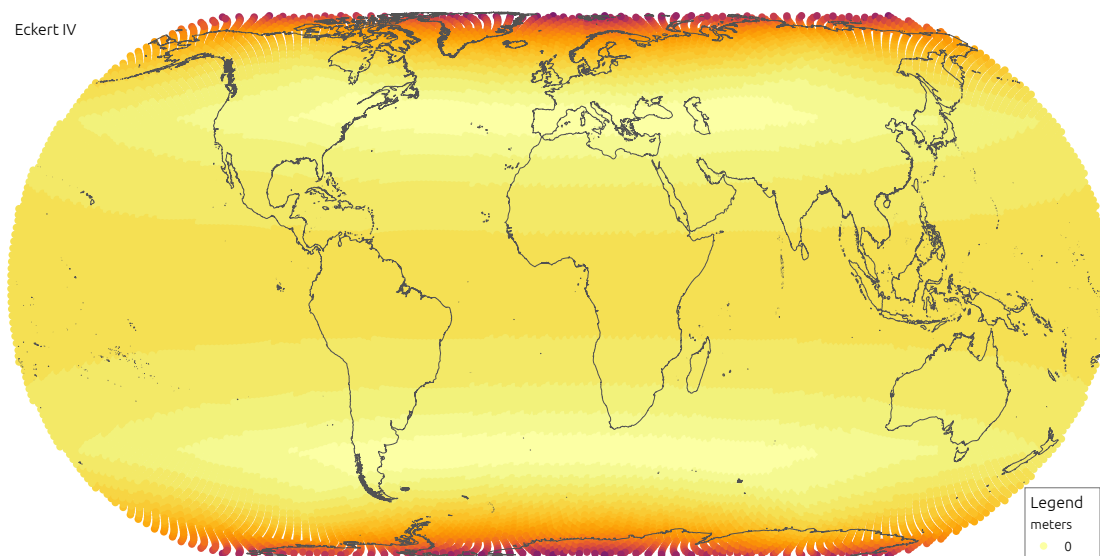


Figure 6. Mean absolute distance distortion at each indicatrix for the Sinusoidal, Mollweide and Hammer projections.

Eckert IV



Homolosine

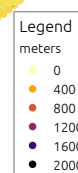
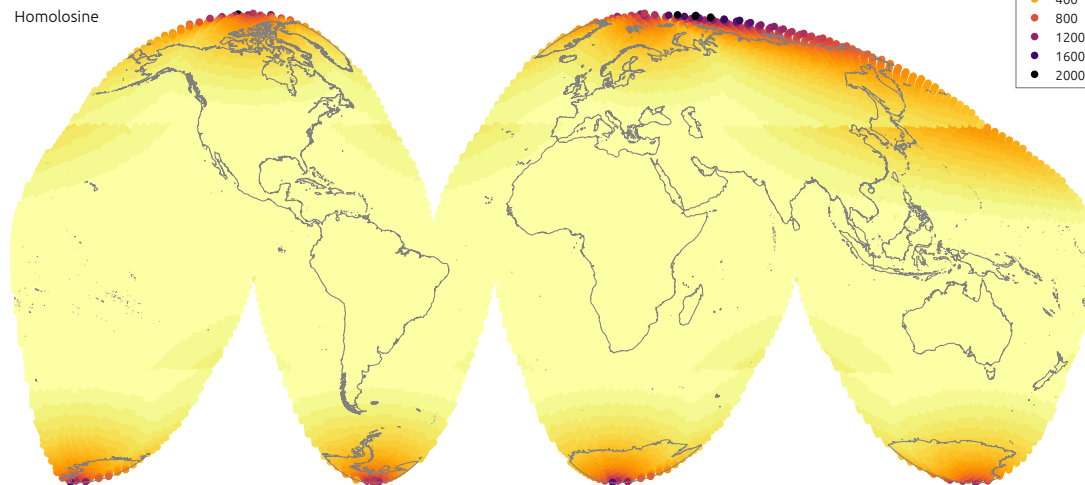


Figure 7. Mean absolute distance distortion at each indicatrix for the Eckert IV and Homolosine projections.

Table 4. Statistics for distance distortions distributions.

(degrees)	Global			Land Masses		
	Mean	RMSE	MAE	Mean	RMSE	MAE
Sinusoidal	380	40,838	380	178	401	178
Mollweide	439	64,168	493	150	348	199
Hammer	298	36,653	415	126	357	197
Eckert IV	590	102,019	693	132	618	237
Homolosine	383	64,153	383	93	200	93

4. Discussion

4.1. Projection Performance

The Sinusoidal projection performs rather well in preserving distances, unsurprisingly, since it is equidistant along parallels. As to angles, it is clearly the worst, with the second highest mean distortion and the highest quantiles. When considering land masses alone, the Sinusoidal retains the poor performance on angles and loses some of the advantage on distances. A marked characteristic of this projection is the uneven spatial distribution of distortions, as they gradually impose with distance from the central point. Land masses like Alaska, Japan or New Zealand are deeply affected, whereas much of Africa and Europe are almost untouched. If the Sinusoidal had an important role in the Cartography of times passed, it comes out as a largely outdated projection in the age of micro-processors.

Even though one of the oldest projections in analysis, the Mollweide performs relatively well. It clearly improves over the Sinusoidal on angles, appearing in the middle of the rank but without imposing too much of a penalty on distances. Distance distortions are ameliorated in land, where the Mollweide appears in the middle of the rank. This is also reflected in the spatial distribution of distortions, which are more relegated to higher latitudes. The Mollweide projection is a classical example of a compromise equal-area formulation, that retains its relevance today. It is still a projection to consider when conveying global data in which both angular and distance accuracy are relevant.

The Hammer projection is unique among those analysed, with distinctive distortions distributions, however, the results it yields are some of the worst. It clearly ranks last in angular distortion but it fails to balance that with a higher performance on distances. The comparison with the ancient Sinusoidal is particularly penalising, the Hammer projection always presents worse distortions. Spatial patterns of distortion are similar to those of the Sinusoidal, with marked differences across continents and oceans. Already when it was first proposed this projection was not among the most performant, it is therefore difficult to justify its use today.

The Eckert IV projection is the most complex to analyse. At face value it appears as a compromise projection, trading angular accuracy for distance distortion, the exact opposite of the Sinusoidal. This is patent in mean distortions, the Eckert IV is close to the Homolosine on angles but is the worst on distances. However, when the analysis is restricted to land masses, distance distortions are less evident and close to those of the Hammer and Mollweide projections. The trade off proposed by the Eckert IV projection is better illustrated by the spatial distribution of distortions. The distortions remain constant across oceans and land, with a sharp increase north of 70° N and south of 70° S. The Eckert IV is perhaps the best replacement for the Homolosine when interruptions may not be so convenient, for instance to work with oceanic or geological data.

The Homolosine shows the best results when considering both the mean or the quantiles of distortions. It is similar to the Sinusoidal for distances and better than EckertIV for angles. When restricting the analysis to land, the advantage of the Homolosine is even more evident, with lower distortions for all measures. The spatial distribution of distortions is also the most even across the five continents, with the largest distortions well consigned to higher latitudes. The main weakness is its focus on land masses, achieved with four more interruptions than the traditional single interruption at

180° E. When working with data covering oceans, for instance, the Homolosine may not be the most appropriate. Especially when computations relying on cell neighbourhood are involved, the additional interruptions imposed by the Homolosine may not be tolerable at all. However, in most cases it is difficult not to select it as the most relevant and performing projection to work with global data on FOSS4G.

Finally, it is important to consider that the projection used at computation time in a big spatial data context may not necessarily match the projection(s) used to present or serve the end result. For instance, a global raster computed on the Homolosine projection may be served through a WCS supporting various projections, even non-equal formulations. Such strategy may be applied when interruptions are deemed applicable to computation but not desirable when presenting results (e.g., to overlay with datasets from other sources).

4.2. Difficulties with FOSS4G

Whereas it was possible to complete this study with FOSS4G, the use of the Homolosine projection is not entirely straightforward. For instance, GDAL supports the projection but the correct application of its inverse requires explicit parametrisation (<https://github.com/OSGeo/gdal/issues/959>). Since programmes using GDAL are not aware of this parametrisation, they generally apply the projection incorrectly in re-projections between different coordinate systems. Therefore any re-projections to and from a coordinate system including the Homolosine projection must always be carried out directly with GDAL.

Cartography FOSS4G programmes (commonly known as “desktop”) present a further obstacle, since they ignore that the co-domain of a map projection is finite in most cases. Therefore, programmes like QGIS or gvSIG portray vector objects spanning over areas that do not have correspondence on the surface of the ellipsoid. To address this problem, a discrete co-domain in vector form was developed that can be used to clean cartograms in such programmes [21].

A particular issue was identified concerning the Sinusoidal projection: the areas of polygons computed in this projection are somewhat different from those obtained with the other projections. Table 5 shows the differences between the Homolosine and the other four projections for the areas of five large countries (computed with QGIS). The Sinusoidal is markedly off, even if the difference is little more than 0.3% of the total area of the geometry. The exact cause has not been identified so far, but this is another reason to avoid using the Sinusoidal projection.

Table 5. Differences in the area of five large countries, respective to the Homolosine projection, computed with QGIS.

Area (km ²)	Sinusoidal	Mollweide	Hammer	Eckert IV
Russia	56,471.34	282.16	352.88	292.54
Canada	28,974.75	−11.11	−7.88	−10.49
China	−19,174.73	1.10	−2.39	5.19
Brasil	−51,327.38	1.23	−0.57	2.74
Australia	−31,999.04	5.06	2.79	7.79

A further problem that affects not only the Homolosine but equal-area projections in general, is the absence of a coordinate system code issued by the European Petroleum Survey Group (EPSG). Programmes like MapServer [22], for instance, do not admit any coordinate system that is not indexed by the EPSG. Even if this issue can be partially addressed by introducing “fake” ESPG codes into the PROJ database, this dependence by OSGeo sanctioned software on the Petroleum industry is something to reflect upon.

Certain hurdles have not yet been overcome, since some programmes simply do not support the Homolosine projection. This is the case with GeoTools [23], for instance. And as it relies on

GeoTools, the popular cloud computing platform Google Earth Engine [24] does not allow the retrieval or computation of datasets in the Homolosine projection.

These remaining issues with FOSS4G are important—but not impairing—and can certainly be resolved; a reminder that FOSS4G requires continuous investment and nurturing.

5. Conclusions and Future Work

This study clearly indicates the Homolosine as the most performant of the equal-area projections analysed. Its interruptions minimise both angular and distance distortions in a way that finds no parallel. To support data primarily related to land masses, the Homolosine is on a league of its own. The International Soil Reference and Information Centre (ISRIC) has recently adopted the Homolosine projection in consequence of these results. In doing so, ISRIC was able to reduce in more than 40% the average computation time required by its global soil mapping framework. In tandem, the size of its global raster maps, produced with a cell side of 250 m, was reduced in more than 1 billion cells. This reduction allowed access to statistics methods that heretofore had not been in reach. The Homolosine projection is also opening the opportunity for ISRIC to further increase the spatial resolution of its reference products.

In general, the results obtained divide the projections considered in two groups: those that maintain relevance today and those that only retain historical interest. Together with the Homolosine, the Mollweide and the Eckert IV projections are worth considering to support global data, all depending on the compromise to strike between accuracy and interruptions. As for the Sinusoidal and Hammer projections, they yield too large and uneven distortions to justify their use in modern times.

The results from this study make clear the advantages of interruptions in equal-area projections: they allow to tackle angular and distance distortions simultaneously. It would therefore be useful to expand support in FOSS4G to other interrupted projections such as the Eumorphic or Snyder's formulations based on the icosahedron and the dodecahedron. Nevertheless, interruptions are not a panacea, they may appear awkward representing a surface that is in fact continuous and, more importantly, may not be suitable to all kinds of analyses or computations. But regarding data portrayal, researchers and data analysts need not to present results on the same projection used to store and analyse data. Simple re-projections (without datum shift) are competently supported by FOSS4G.

Various of the projections assessed attempt to minimise distortion on land masses and all yield high distortions in the polar regions. In some cases, like the Homolosine and the Eckert IV, this is intentional. In this study the intersection of the equator with the Greenwich meridian was used as the central point of projection. It is therefore worth asking whether this point is optimal. A further study could focus on this question, particularly relevant for the single interruption projections.

Finally, it is useful to consider cartography beyond planet Earth. Projections like the Homolosine or the Eumorphic include ad hoc interruptions aligned with the oceans and continents of Earth. As increasingly more data is collected in other planets of the solar system, it is relevant to revisit this kind of projections and develop interruptions that may apply more universally.

Author Contributions: L.M.d.S. conceptualised the study, developed the software and lead the redaction of the manuscript. L.P. tested the use of the Homolosine projection with FOSS4G, contributed to the statistical summary of results and reviewed/edited the manuscript. B.K. contributed with project management, study conception and manuscript review/edition.

Funding: This research received no external funding

Conflicts of Interest: The authors declare no conflict of interest.

References

1. GRASS Development Team. GRASS: Geographic Resources Analysis Support System. Open Source Geospatial Foundation Project. 2019. Available online: <https://grass.osgeo.org/> (accessed on 8 August 2019).
2. Snyder, J.P. An equal-area map projection for polyhedral globes. *Cartographica* **1992**, *29*, 10–21. [CrossRef]

3. Karney, C.F.F. GeographicLib Version 1.49. 2017. Available online: <https://geographiclib.sourceforge.io> (accessed on 8 August 2019).
4. PROJ Contributors. PROJ Coordinate Transformation Software Library. 2019. Available online: <https://proj4.org/> (accessed on 08 August 2019).
5. GDAL/OGR Contributors. GDAL/OGR Geospatial Data Abstraction Software Library. 2019. Available online: <http://gdal.org> (accessed on 08 August 2019).
6. Seong, J.C.; Mulcahy, K.A.; Usery, E.L. The sinusoidal projection: A new importance in relation to global image data. *Prof. Geogr.* **2002**, *54*, 218–225. [[CrossRef](#)]
7. Capek, R. Which is the best projection for the world map. *Proc. Int. Cartogr. Conf.* **2001**, *5*, 3084–3093.
8. Mulcahy, K.A.; Clarke, K.C. Symbolization of map projection distortion: A review. *Cartogr. Geogr. Inf. Sci.* **2001**, *28*, 167–182. [[CrossRef](#)]
9. De Sousa, L.M. Remaining gaps in open source software for Big Spatial Data. Technical report. *PeerJ Prepr.* **2018**. [[CrossRef](#)]
10. QGIS Development Team. QGIS Geographic Information System. 2019. Available online: <https://qgis.org> (accessed on 8 August 2019).
11. Anguix, A.; Díaz, L. gvSIG: A GIS desktop solution for an open SDI. *J. Geogr. Reg. Plan.* **2008**, *1*, 041–048.
12. Eckert, M. Neue Entwürfe für Erdkarten. *Petermanns Geogr. Mitteilungen (Gotha)* **1906**, *52*, 97–109.
13. Craster, J. Some equal-area projections of the sphere. *Geogr. J.* **1929**, *74*, 471–474. [[CrossRef](#)]
14. Goode, J.P. The Homolosine projection: A new device for portraying the Earth's surface entire. *Ann. Assoc. Am. Geogr.* **1925**, *15*, 119–125. [[CrossRef](#)]
15. Hammer, E.H.H. Über die Planisphäre von Aitow und verwandte Entwürfe, insbesondere neue flächentreue iihnlicher Art. *Petermanns Geogr. Mitteilungen (Gotha)* **1892**, *38*, 85–87.
16. Snyder, J.P. *Flattening the Earth: Two Thousand Years of Map Projections*; University of Chicago Press: Chicago, IL, USA, 1997.
17. Tissot, N.A. *Mémoire sur la Représentation des Surfaces et les Projections des Cartes Géographiques*; Gauthier-Villars: Paris, France, 1881.
18. Kraak, M.; Ormeling, F. *Cartography: Visualization of Spatial Data*, 3rd ed.; chapter Data Acquisition; Prentice Hall: Upper Saddle River, NJ, USA, 2009.
19. Sahr, K.; White, D.; Kimerling, A.J. Geodesic Discrete Global Grid Systems. *Cartogr. Geogr. Inf. Sci.* **2003**, *30*, 121–134. [[CrossRef](#)]
20. Barnes, R.; Sahr, K.; Evenden, G.; Johnson, A.; Warmerdam, F. dggridR: Discrete Global Grids for R. 2016. Available online: <https://github.com/r-barnes/dggridR/> (accessed on 8 August 2019).
21. De Sousa, L.M. Vectors for Goode's Homolosine Projection. *Zenodo* **2018**, doi:10.5281/zenodo.1841337. [[CrossRef](#)]
22. Lime, S. MapServer. In *Open Source Approaches in Spatial Data Handling*; Springer: Berling, Germany, 2008; pp. 65–85.
23. Turton, I. GeoTools. In *Open Source Approaches in Spatial Data Handling*; Springer: Berling, Germany, 2008; pp. 153–169.
24. Gorelick, N.; Hancher, M.; Dixon, M.; Ilyushchenko, S.; Thau, D.; Moore, R. Google Earth Engine: Planetary-scale geospatial analysis for everyone. *Remote Sens. Environ.* **2017**, *202*, 18–27. [[CrossRef](#)]

